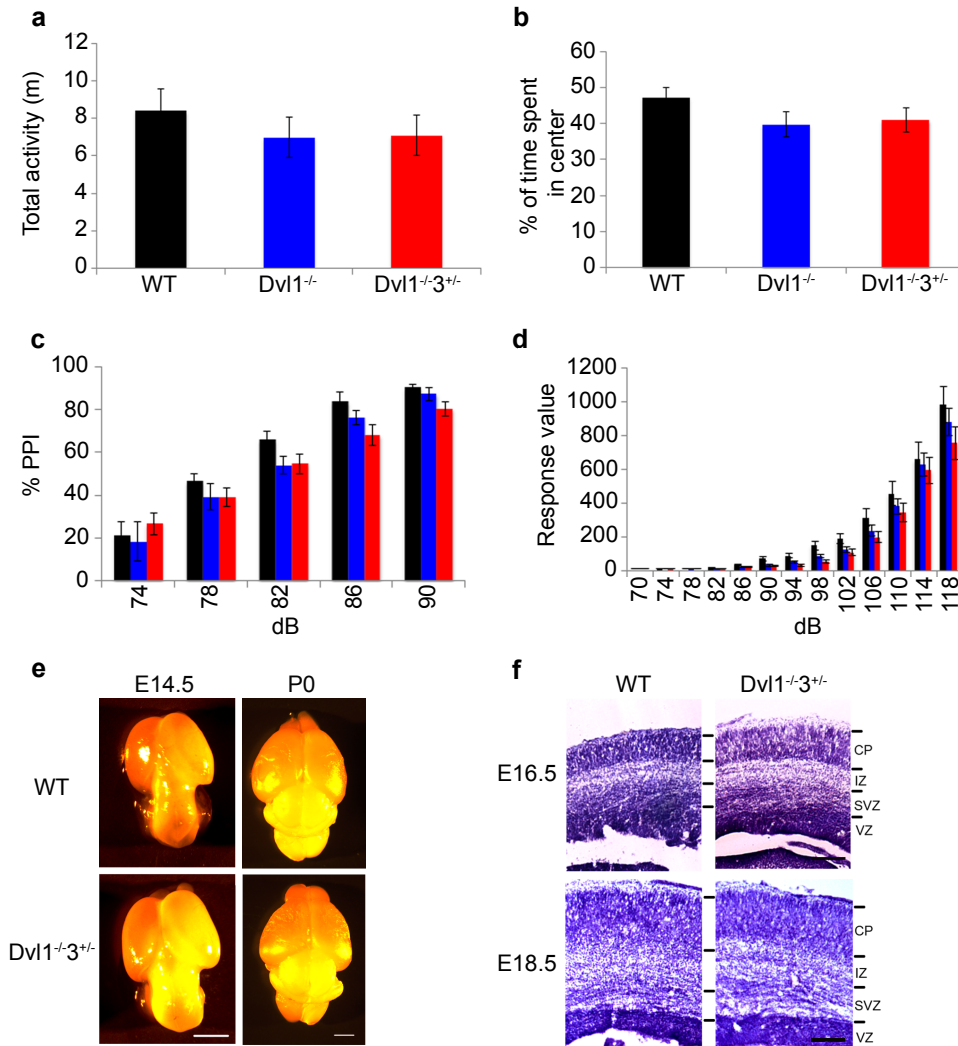


**Supplementary Materials:
Supplementary Table 1**

		WT (n=11)	Dvl1 ^{-/-} (n=12)	Dvl1 ^{-/-3+/-} (n=12)
	Age	3.9±0.1	3.8±0.1	3.9±0.1
	Background	129	129	129
	Male/Female	6/5	7/5	4/8
Gross behavioral assessment	Wild Running	No	No	No
	Excessive Grooming	No	No	No
	Freezing	No	No	No
	Rearing	Yes	Yes	Yes
	Jumping	No	No	No
	Defecation	Normal	Normal	Normal
	Urination	Normal	Normal	Normal
	Explore Entire Cage	Yes	Yes	Yes
	Hunched	No	No	No
Gross physical assessment	Fur Color	Agouti	Agouti	Agouti
	Dirty Fur	No	No	No
	Ulcerated Skin	No	No	No
	Bald Spots	No	No	No
	Thinning Hair	No	No	No
	Labored Breaths	No	No	No
	Piloerection	No	No	No
	Nose	Good	Good	Good
	Teeth	Good	Good	Good
	Nails	Good	Good	Good
	Rectum	Good	Good	Good
sensorimotor reflexes	Approaching Object	Normal	10/11 Normal	Normal
	Eye Blink Reflex	Normal	Normal	Normal
	Palpebral Closure	No	No	No
	Exophtalmias	No	No	No
	Ear Twitch Reflex	Normal	Normal	Normal
	Whisker Reflex	Normal	Normal	Normal
Postural Reflexes	Upright Posture	immediatly	immediatly	immediatly
	Balance	Maintain	Maintain	Maintain balance
	Tail Suspension	Normal	Normal	Normal

Supplementary Table 1: Gross behavioral, physical and reflexes assessment. WT, Dvl1^{-/-} and Dvl1^{-/-3+/-} mice were individually assessed and scored for gross behavioral, physical and reflexes.



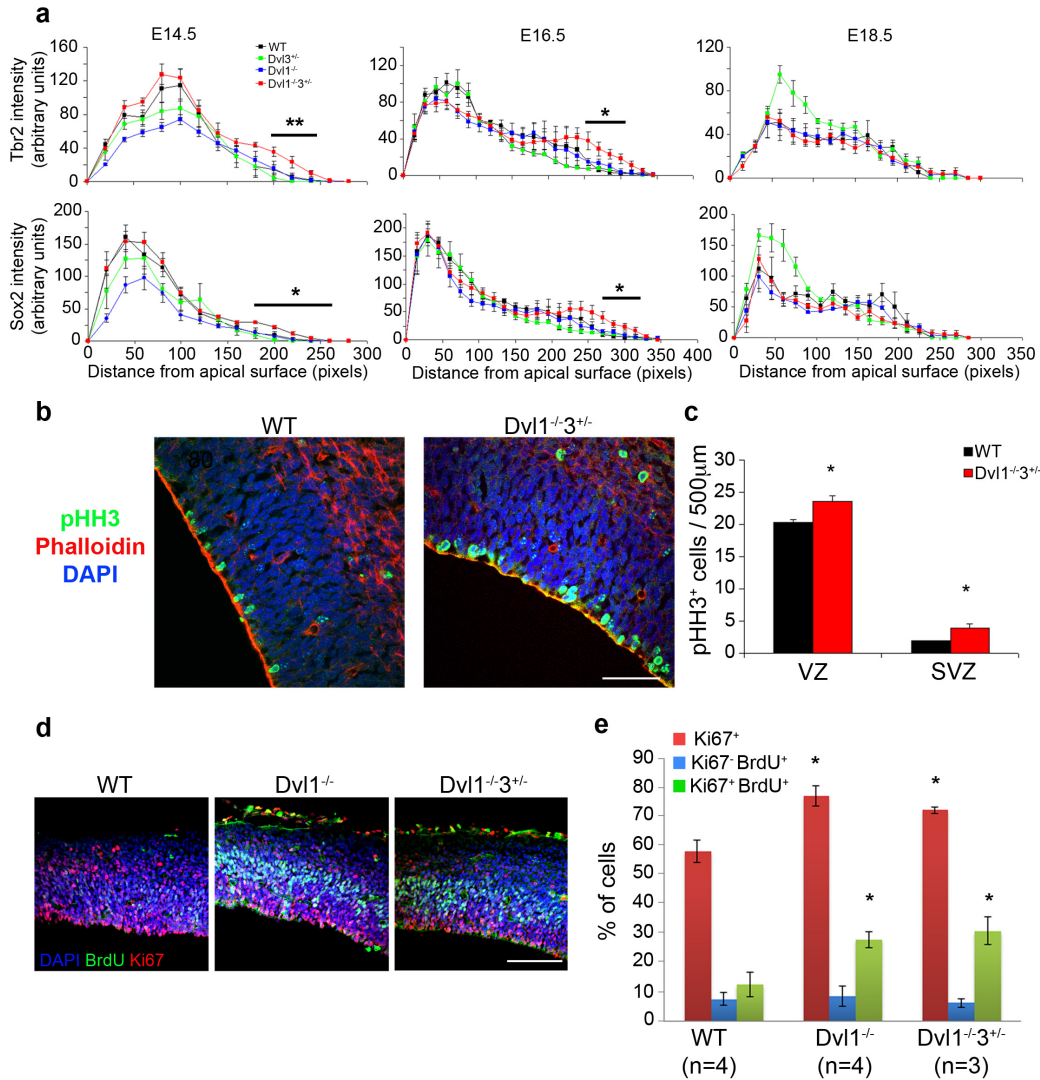
Supplementary Fig. 1: *Dvl1*^{-3+/-} mutants Behavioral examination and embryonic brain enlargement. The open field task was performed on WT and *Dvl* mutant mice and the total distance traveled (**a**), and the time spent in the center of the arena relative to their total activity (**b**) are presented as mean±SEM. **c**, pre-pulse inhibition task was performed on WT and *Dvl* mutant mice and response values are presented as mean±SEM. **d**, Acoustic startle response was performed on WT and *Dvl* mutant mice and response values are presented as mean±SEM. **e**, Representative images of whole brains of WT and *Dvl1*^{-3+/-} embryos at E14.5 and P0 (scale bar: 1mm). **f**, Representative images of the neocortex from Nissl stained sections are shown of WT and *Dvl1*^{-3+/-} embryos at E12.5, E16.6 and E18.5 (scale bar: 100µm).

Supplementary Table 2

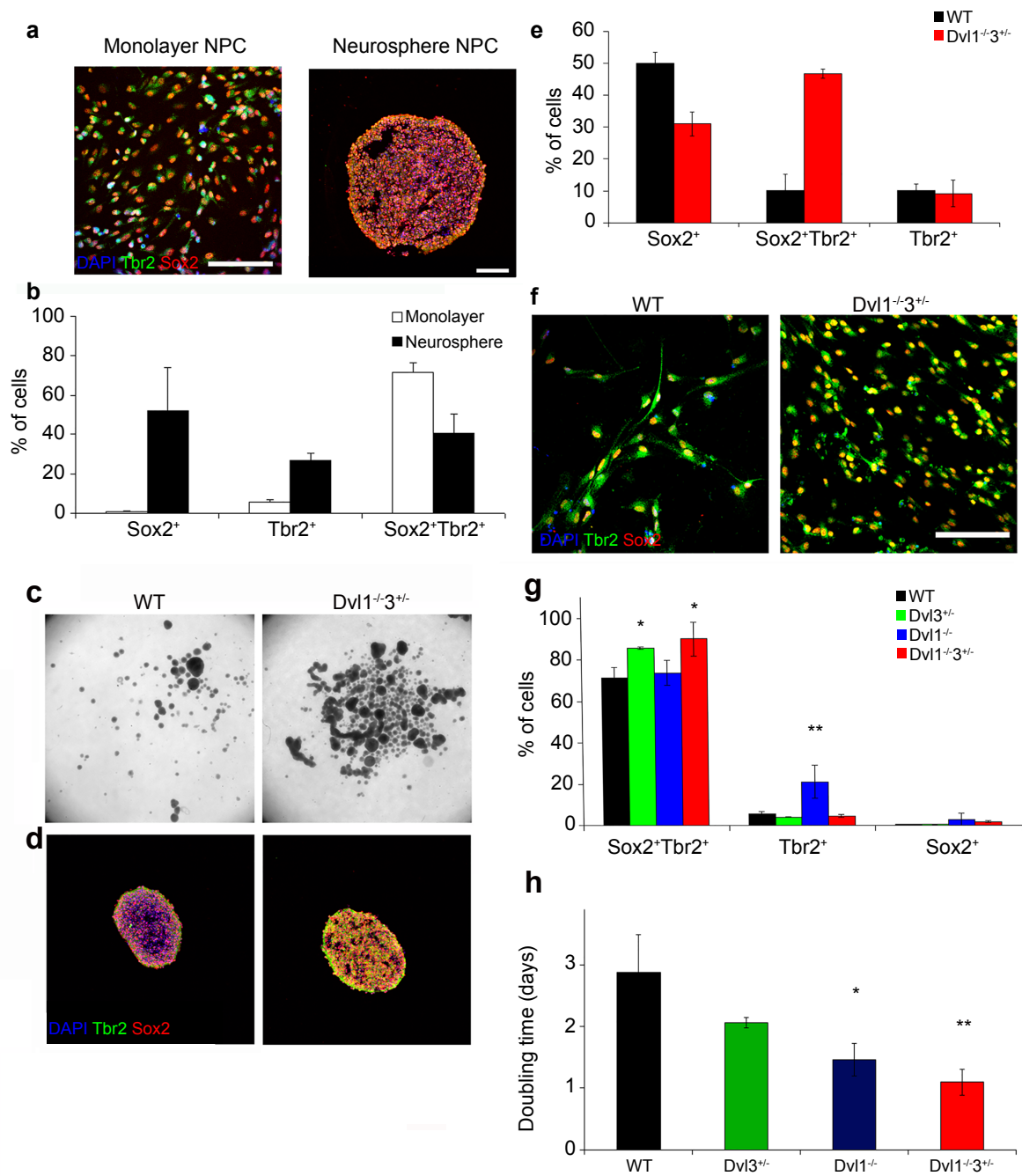
	Embryonic Day	WT	<i>Dvl3</i> ^{+/-}	<i>Dvl1</i> ^{-/-}	<i>Dvl1</i> ^{-/-3} ^{+/-}
Head weight (mg)	E12.5	18.65 ± 0.92 (n=7)	18.56 ± 1.53 (n=3)	16.87 ± 3.91 (n=4)	14.28 ± 0.88 (n=5)
Brain weight (mg)	E14.5	21.13 ± 1.1 (n=9)	24.41 ± 0.60 (n=15)	22.42 ± 1.29 (n=14)	26.86 ± 2.33 * (n=6)
	E16.5	47.93 ± 2.21 (n=3)	50.16 ± 1.04 (n=8)	44.96 ± 1.16 (n=5)	45.71 ± 1.81 (n=6)
	E18.5	70.48 ± 2.33 (n=4)	64.63 ± 4.82 (n=3)	73.15 ± 1.24 (n=10)	66.25 ± 2.77 (n=4)
	P0	117.74 ± 10.14 (n=5)	106.80 ± 6.89 (n=4)	104.65 ± 4.75 (n=3)	98.50 ± 3.06 (n=5)
Neocortex width (pixel)	E12.5	81.8 ± 0.84	81.69 ± 2.01	79.19 ± 2.27	74.59 ± 1.46
	E13.5	113.3 ± 5.99	107.49 ± 3.56	107.36 ± 1.67	103.47 ± 4.86
	E14.5	149.60 ± 6.32	161.61 ± 5.08	200.19 ± 12.30*	194.56 ± 12.94 *
	E16.5	298.31 ± 5.04	277.62 ± 9.11	261.08 ± 16.48	292.75 ± 9.39
	E18.5	322.25 ± 8.56	259.94 ± 5.27	303.03 ± 16.13	324.47 ± 6.92
VZ width (pixel)	E12.5	66.82 ± 0.45	70.13 ± 1.39	67.70 ± 1.64	63.05 ± 1.01
	E13.5	89.76 ± 5.17	85.39 ± 3.54	85.99 ± 2.27	82.65 ± 3.95
	E14.5	71.04 ± 1.39	73.88 ± 2.74	88.33 ± 8.89	83.07 ± 7.43
	E16.5	76.89 ± 1.82	61.60 ± 1.35	60.40 ± 1.69	66.07 ± 2.65
	E18.5	62.59 ± 4.81	51.68 ± 4.08	48.14 ± 5.94	55.43 ± 1.08
CP width (pixel)	E12.5	14.98 ± 0.84	11.56 ± 0.77	11.50 ± 0.66	11.54 ± 0.59
	E13.5	22.72 ± 1.59	22.10 ± 0.61	21.37 ± 0.89	20.82 ± 1.04
	E14.5	23.06 ± 2.88	25.60 ± 1.59	27.40 ± 1.67	34.18 ± 2.20 **
	E16.5	88.23 ± 2.57	88.70 ± 8.26	84.13 ± 4.10	98.53 ± 6.30
	E18.5	128.85 ± 5.29	101.70 ± 11.18	109.26 ± 8.93	117.38 ± 7.54

Supplementary Table 2: Embryonic brain weight and size across developmental stages.

Whole brains of WT, *Dvl3*^{+/-}, *Dvl1*^{-/-} and *Dvl1*^{-/-3}^{+/-} embryos, from at least three litters per time point, were dissected between E12.5 and P0 and weighed on an analytical scale and is presented as mean±SEM, (ANOVA<0.001 *p<0.04 for comparing the results of *Dvl1*^{-/-3}^{+/-} with those of WT embryos). For width analysis, brain embryos were dissected between E12.5 and E18.5, prepared for histology, sectioned and stained by cresyl-violet. Sections were photographed and images were measured for widths of the neocortex, ventricular zone (VZ) and cortical plate (CP) widths. Widths are presented as mean±SEM. (ANOVA<0.02 *p<0.02; ** p<0.03 for comparing the results of *Dvl1*^{-/-3}^{+/-} with those of WT embryos).

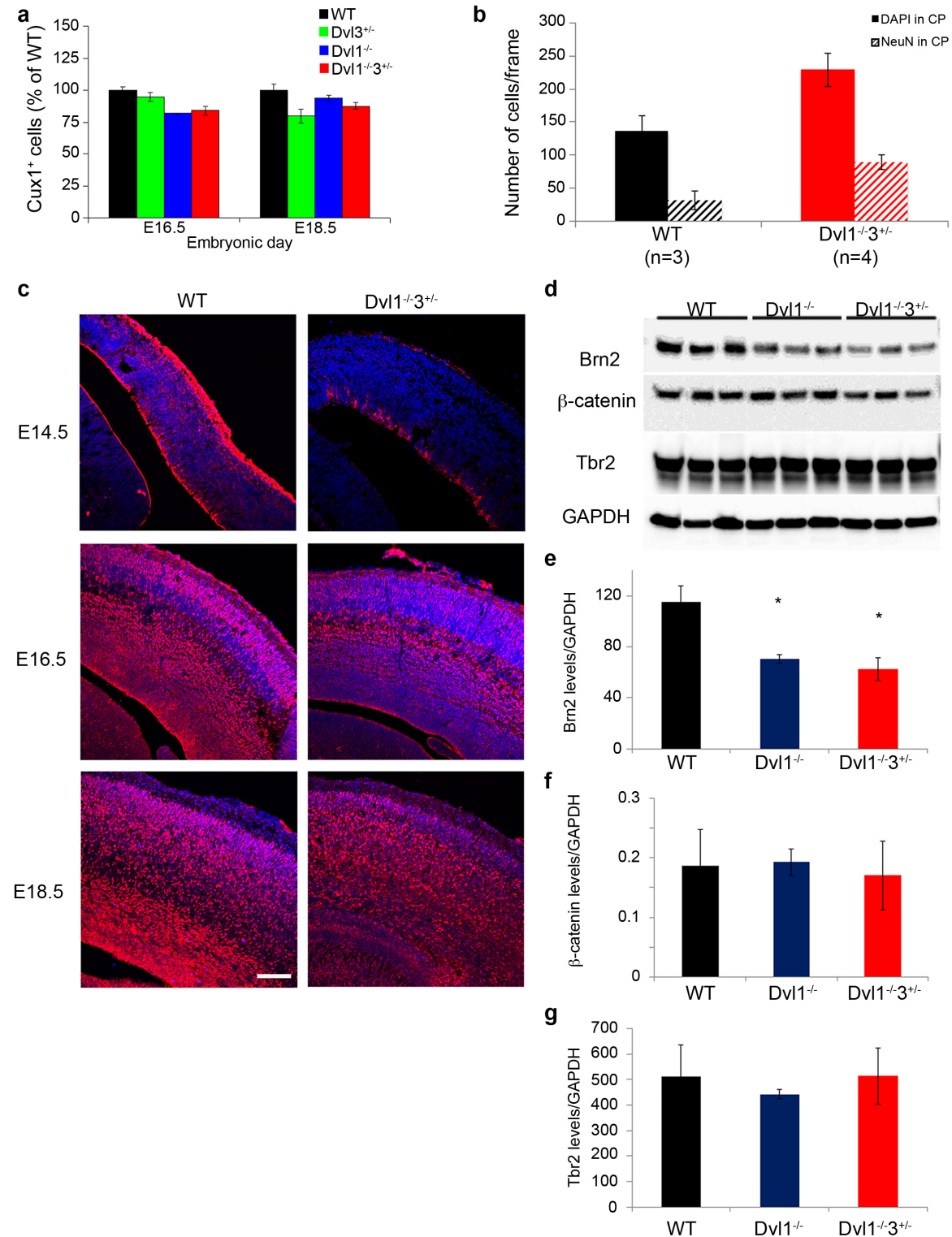


Supplementary Fig. 2: Genetic loss of *Dvl1* and *Dvl3* induces basal progenitor expansion. **a**, Coronal sections of WT and *Dvl1*^{-3^{+/+}} mutant embryo were double labeled with anti-Sox2 and anti-Tbr2. Quantification of individual stain intensities along the apical-basal axis of the cerebral cortex were analyzed at the indicated time points. Intensities are presented as mean±SEM of n=3-5 per group (**p<0.03 and *p<0.05 for comparing the results of the *Dvl1*^{-3^{+/+}} with those of the other genotypes). **b**, Triple-label confocal microscopy using DAPI (blue), anti-pHH3 (green) and phalloidin-594 (red) at E14.5 (scale bar=50µm). **c**, Quantification of the levels of pHH3⁺ cells are presented as mean±SEM of n=4 per group (*p<0.04 for comparing the results of the *Dvl1*^{-3^{+/+}} with those of the WT embryos). Black and red bars represent WT and *Dvl1*^{-3^{+/+}} genotypes, respectively. **d**, Triple-label confocal microscopy using DAPI (blue), anti-BrdU (green) and anti-Ki67 (red) at E14.5 (scale bar=100µm). **e**, Quantification of the levels of Ki67⁺ (red bars), Ki67⁻ BrdU⁺ (blue bars) and Ki67⁺ BrdU⁺ (green bars) cells are presented as mean±SEM of (*p<0.04 for comparing the results of the *Dvl1*^{-/-} and *Dvl1*^{-3^{+/+}} with those of the WT embryos).



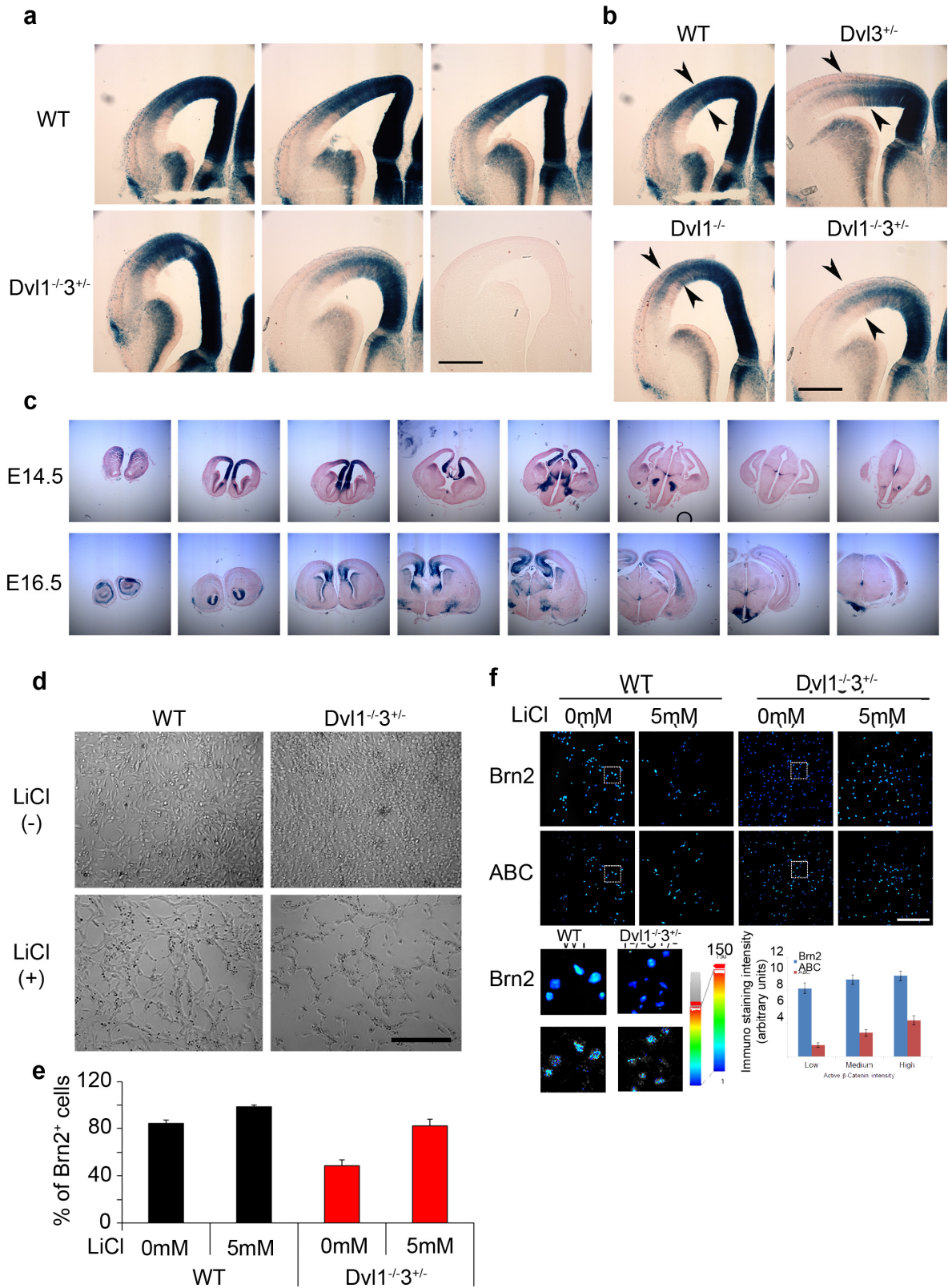
Supplementary Fig. 3: NPC culture conditions govern their apical/basal characteristics. **a**, NPCs cultured as adherent monolayers and neurospheres were fixed and double labeled with anti-Sox2 and anti-Tbr2. **b**, The single and double labeled cells in each culture condition were quantified as the percentage of total cells (mean±SEM of n=3 per group). White and black bars represent monolayer and neurosphere culture conditions, respectively. **c**, Cortical NPCs of WT and *Dvl* mutant mice were cultured as neurospheres (NS) and representative image of NS formation is presented. **d**, NS were sectioned and labeled with DAPI (Blue), anti-Sox2 (Red) and anti-Tbr2 (Green). Representative images are shown

(scale bar: 100 μ m). **e**, Sox2 and Tbr2 single and double labeled cells in NS were quantified as the percentage of the total cells counted (DAPI). Results are presented as mean \pm SEM (n \geq 3, *p<0.01 for comparing the percentage of double labeled Sox2⁺Tbr2⁺ cells in the *Dvl1*^{-/-}*3*^{+/-} NS with those of the WT NS. **f**, Cortical NPCs of WT and *Dvl* mutant mice were cultured as adherent monolayer and labeled with DAPI (Blue), anti-Sox2 (Red) and anti-Tbr2 (Green). Representative images are shown (scale bar: 100 μ m). **g**, Sox2 and Tbr2 single and double labeled cells in adherent monolayer culture were quantified as the percentage of the total cells counted (DAPI). Results are presented as mean \pm SEM (n \geq 3, ANOVA<0.001 *p<0.02 for comparing the percentage of double labeled Sox2⁺Tbr2⁺ cells in the *Dvl1*^{-/-}*3*^{+/-} and *Dvl3*^{+/-} NPCs with those of the WT NPCs and ANOVA<0.001 **p<0.04 for comparing the percentage of double labeled Tbr2⁺ cells in the *Dvl1*^{-/-} NPCs with those of all the NPCs groups). **h**, Adherent monolayer NPCs from WT and *Dvl* mutant embryos were dissociated, counted for calculation of population doubling time. Results are presented as mean \pm SEM, ANOVA<0.05 *p<0.05 and **p<0.02 for comparing the doubling time of the *Dvl1*^{-/-} and *Dvl1*^{-/-}*3*^{+/-} NPCs respectively with those of the WT NPCs). Black, green, blue and red bars represent WT, *Dvl3*^{+/-}, *Dvl1*^{-/-} and *Dvl1*^{-/-}*3*^{+/-} genotypes, respectively.



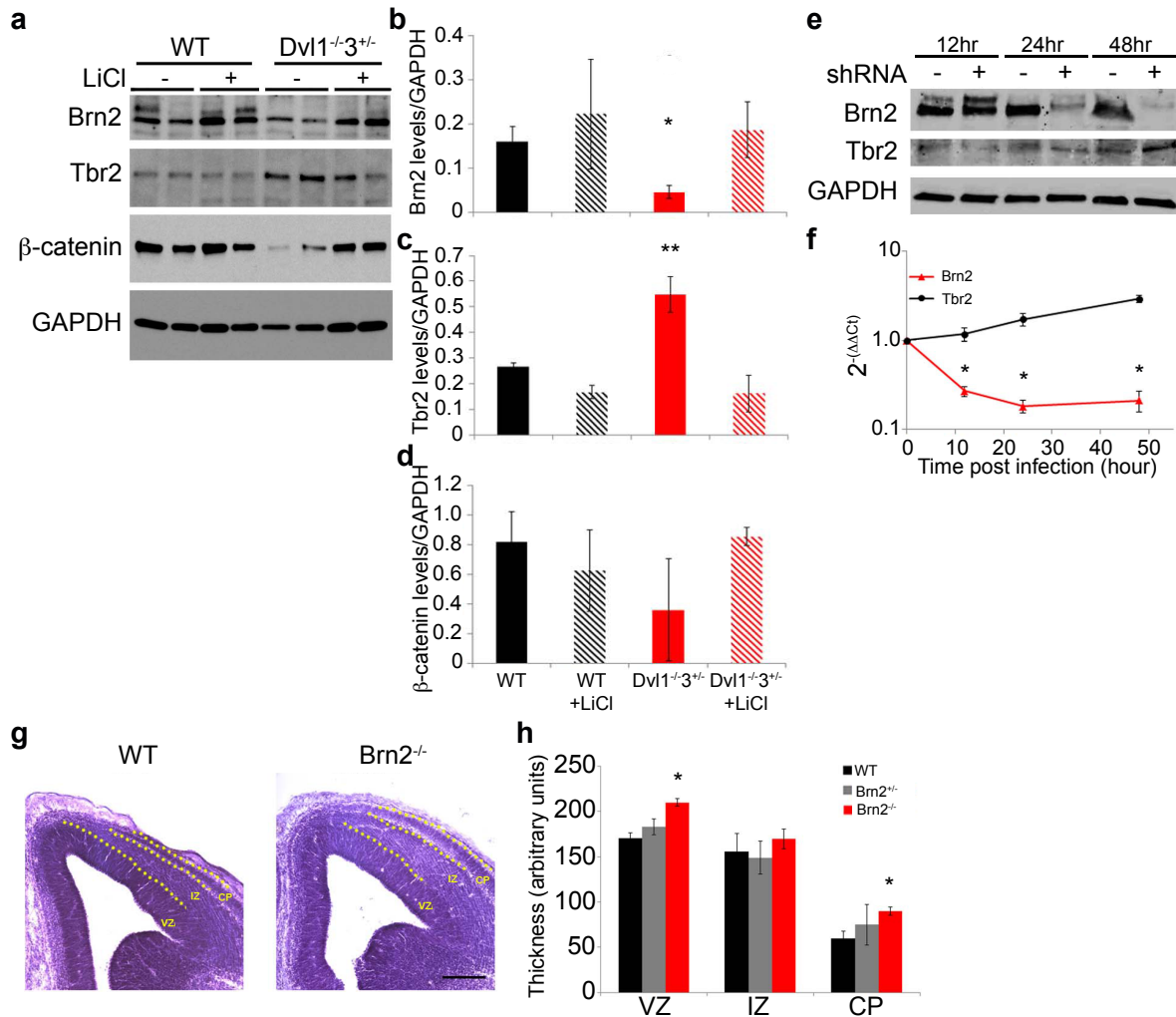
Supplementary Fig. 4: Dvl loss induces deregulation of Brn2 levels in the developing cortex. **a**, Coronal sections of WT and *Dvl* mutant embryonic brains were stained with anti-Cux1, a superficial layer neuron marker (see Fig. 3a). Quantification of the percentage of Cux1⁺ neurons at the indicated time point is presented (mean±SEM). **b**, Coronal sections of WT and *Dvl* mutant embryonic

brains at E14.5 were stained with anti-NeuN (see Figure 3c). Quantification of the percentage of NeuN⁺ neurons at E14.5 is presented (mean±SEM) *p<0.05 for comparing the number of DAPI⁺ and NeuN⁺ cells in the *Dvl1*^{-/-}*3*^{+/-} embryos with those of the WT embryo. **c**, Representative images of coronal sections from WT and *Dvl1*^{-/-}*3*^{+/-} brains double-labeled with DAPI (blue) and Brn2 (red) at E14.5, E16.5 and E18.5 (scale bar=100µm). **d**, E14.5 frontal cortices of WT and *Dvl* mutant were dissected, lysed and immunoblots were performed with anti-Brn2, anti-Tbr2, anti-β-catenin and GAPDH. Immunoblots were quantified (**e-g**) as relative expression to GAPDH expression. Results are presented as mean±SEM (n≥3, ANOVA<0.05 *p<0.04 for comparing the results of the *Dvl* mutants with those of the WT). Black, green, blue and red bars represent WT, *Dvl3*^{+/-}, *Dvl1*^{-/-} and *Dvl1*^{-/-}*3*^{+/-} genotypes, respectively.



Supplementary Fig. 5: reduced β -catenin transcriptional activity controls the regulation of Brn2 levels in NPCs. a, Representative images of X-gal staining of

brains from WT and *Dvl1^{-/-}3^{+/-}* BAT-Gal embryos (scale bar: 250 μ m). **b**, Brains from WT and *Dvl* mutant BAT-Gal embryos were sectioned and X-gal staining was performed. Representative images are shown of the neocortex of WT, *Dvl3^{+/-}*, *Dvl1^{-/-}* and *Dvl1^{-/-}3^{+/-}* embryos from E14.5 (scale bar: 250 μ m). **c**, Representative images of X-gal staining of brains from WT BAT-Gal embryos at E14.5 and E16.5 (scale bar: 1mm). **d**, WT and *Dvl1^{-/-}3^{+/-}* NPCs that were treated with 5mM LiCl for 3 days and representative phase contrast images are presented (Scale bar: 100 μ m). **e**, Monolayer adherent NPCs from WT and *Dvl1^{-/-}3^{+/-}* embryos were treated with 5mM LiCl for 3 days and stained with anti-Brn2 (see Fig. 4e). Quantification of the percentage of Brn2⁺ cells is presented (mean \pm SEM) *ANOVA<0.03; p<0.01 for comparing the percentage of Brn2⁺ cells in the *Dvl1^{-/-}3^{+/-}* NPCs with those of the WT NPCs. **f**, Monolayer adherent NPCs from WT and *Dvl1^{-/-}3^{+/-}* embryos were treated with 5mM LiCl and stained with anti-Brn2 and anti-ABC (active form of β -catenin). **Upper panel**: Representative Brn2 and ABC pseudo-colored images. **Left lower panel**: Higher magnification views of the WT and *Dvl1^{-/-}3^{+/-}* NPCs that are marked in the upper panel by red squares. **Right Lower Panel**: Quantification of the Brn2 (blue) and ABC (red) average intensities divided into low medium and high expressing ABC cells. Results from WT and *Dvl1^{-/-}3^{+/-}* were combined and are presented as mean \pm SEM of n=3-5 per group.

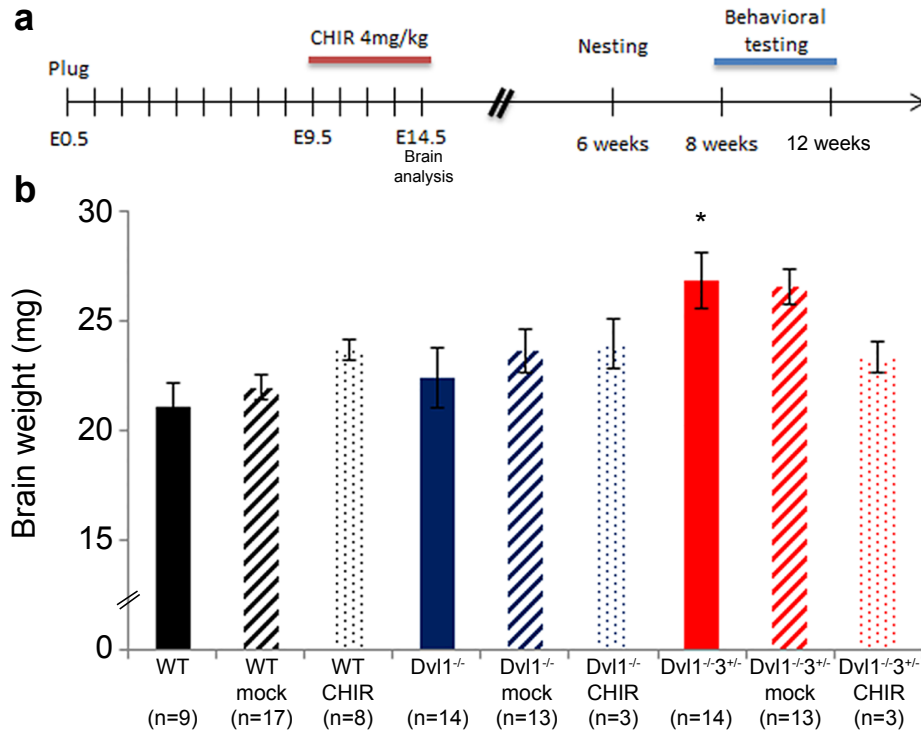


Supplementary Fig. 6: Brn2 direct regulation of Tbr2 levels. **a**, Monolayer adherent NPCs were treated with LiCl and immunoblots were performed with anti-Brn2, anti-Tbr2, anti-β-catenin and GAPDH. A representative blot from 3 independent experiments is presented. **b-d**, Immunoblots were quantified as relative expression to GAPDH expression. Results are presented as mean±SEM (n≥3, ANOVA<0.05 *p<0.05 for comparing the results of the *Dvl1*^{-3+/-} mock treated with those of the *Dvl1*^{-3+/-} LiCl treated and WT mock treated; ANOVA<0.002 **p<0.01 for comparing the results of the *Dvl1*^{-3+/-} LiCl treated with those of the other mouse groups. **e-f**, Adherent WT NPCs grown as monolayer culture were infected with shRNA for Brn2 or GFP. Protein and RNA was extracted from the cells at 12, 24 and 48 hours post infection, and the levels of Brn2 and Tbr2 were measured using immunoblots and RT-PCR (*p<0.01 for comparing the results of the infected cells to the non infected cells). **g-h**, Brains of WT and *Brn2* E14.5 mutant embryos were sectioned and Nissl staining was performed. Representative images are shown of the neocortex of WT and *Brn2*^{-/-} embryos (scale bar: 100μm). **h**, The widths of the neocortex regions were measured. Results are presented as mean±SEM (n≥4, ANOVA<0.02 *p<0.03 for comparing the results of the *Brn2*^{-/-} embryonic brains with those of the WT brains). Black, gray and red bars represent WT *Brn2*^{+/-} and *Brn2*^{-/-} genotypes, respectively.

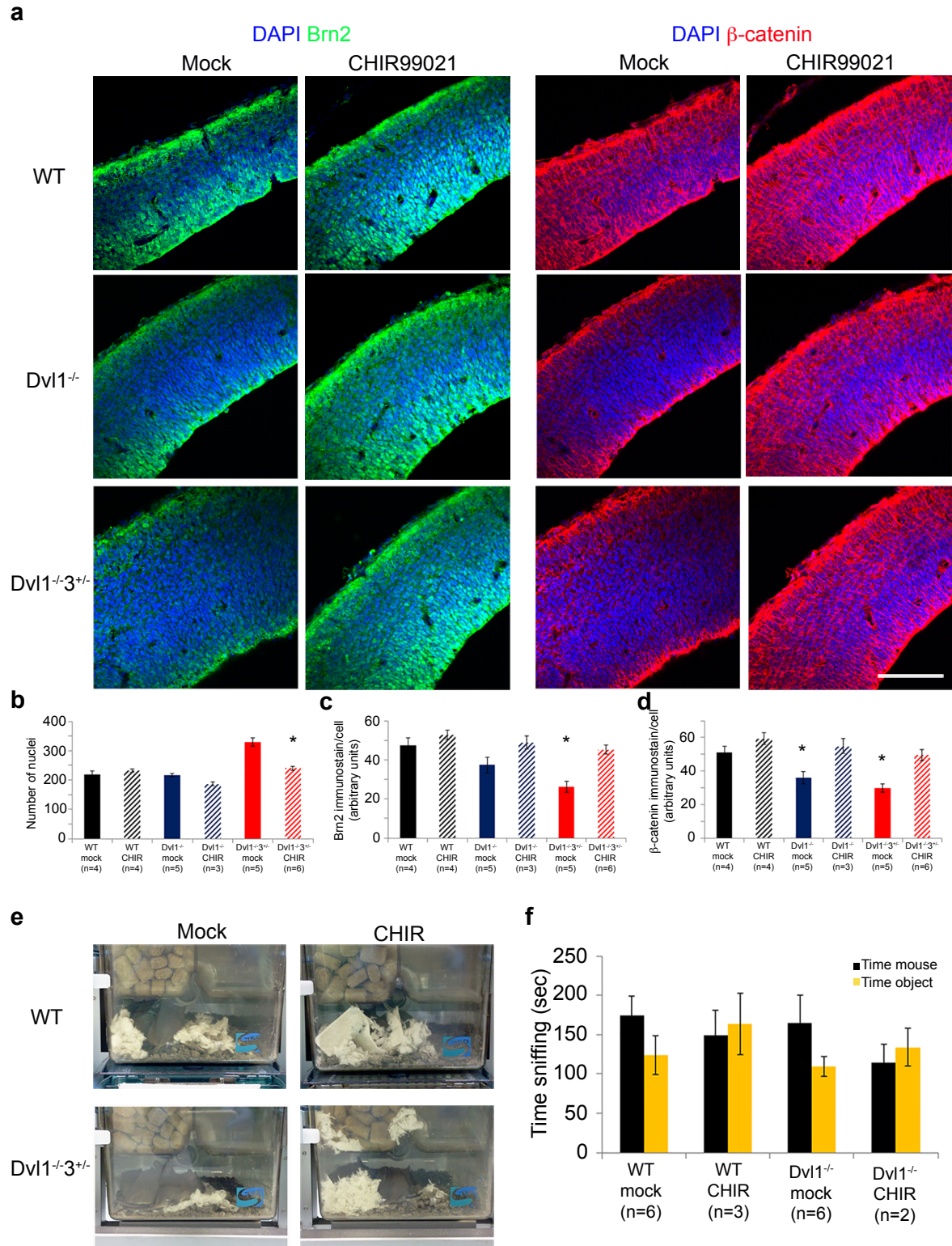
Supplementary Table 3

	Embryonic Day	WT	<i>Brn2</i> ^{+/-}	<i>Brn2</i> ^{-/-}
Neocortex width (pixel)	E14.5	393.29 ± 10.76	407.30 ± 44.11	469.86 ± 26.86*
VZ width (pixel)	E14.5	170.60 ± 5.88	183.27 ± 20.21	209.92 ± 8.52*
IZ width (pixel)	E14.5	155.77 ± 8.74	149.08 ± 18.45	169.76 ± 22.22
CP width (pixel)	E14.5	59.63 ± 4.35	74.95 ± 10.71	90.18 ± 4.60

Supplementary Table 3: Measurement of size of neocortical areas across developmental stages. Whole brains of WT, *Dvl3*^{+/-}, *Dvl1*^{-/-} and *Dvl1*^{-/-}*3*^{+/-} embryos, from 4 litters were dissected at E14.5. For width analysis, brains WT, *Brn2*^{+/-} and *Brn2*^{-/-} embryos were, prepared for histology, sectioned and stained by cresyl-violet (see experimental design). Sections were photographed and images were measured for widths of the cortical wall, the VZ, IZ and the CP by using ImagePro plus ver.6.0. Width is presented as mean±SEM. (ANOVA<0.02 *p<0.04 for comparing the results of *Brn2*^{-/-} with those of WT embryos).

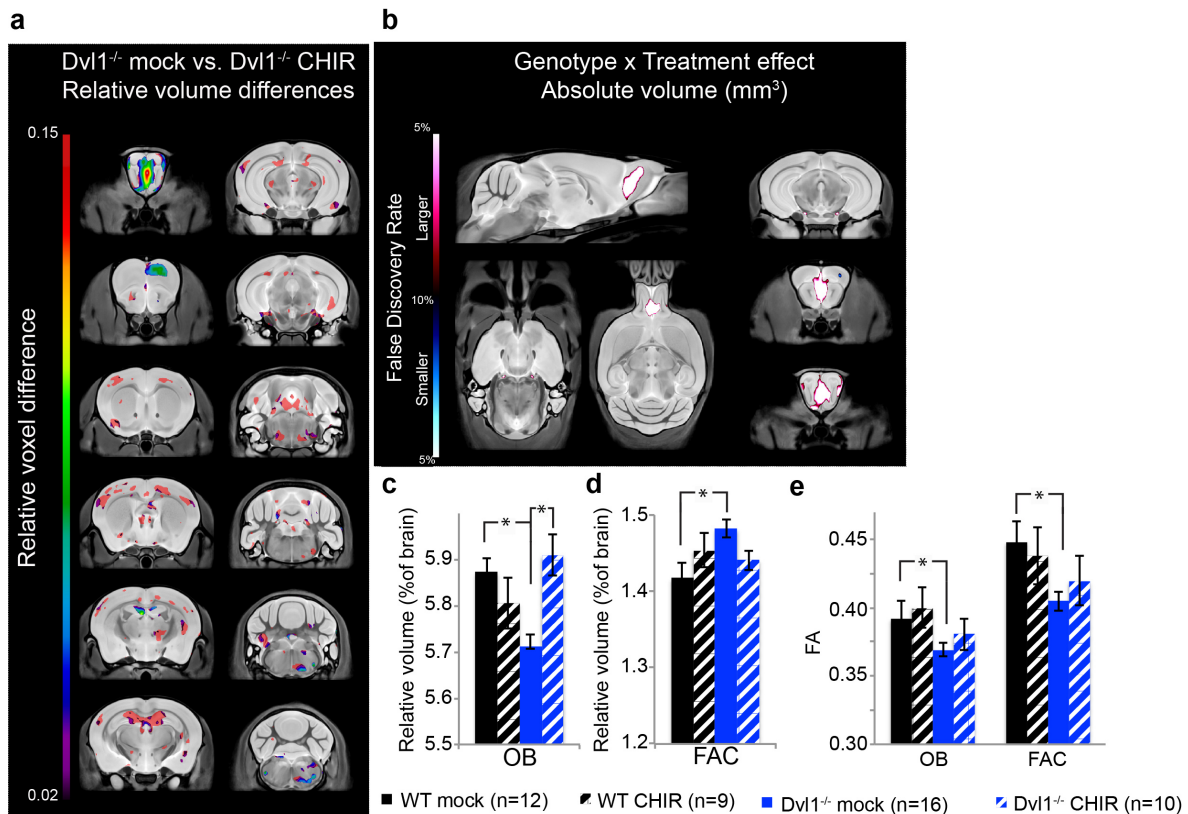


Supplementary Fig. 7: Embryonic activation of Wnt canonical pathway rescue brain over growth. **a**, Schematic representation of the experimental design. Pregnant Dams were injected daily from E9.5-E14.5 with CHIR99021 (4mg/kg). Pups were separated by gender and genotype at weaning. At 6 weeks of age mice were tested for nesting and at 8-12 weeks tested in the open field, three chamber social approach task and marble burying. **b**, Brains (E14.5) of WT and *Dvl* mutant embryos that were CHIR99021 or mock treated were weighed on an analytical scale. (mean±SEM, ANOVA<0.02 *p<0.04 for comparison of the *Dvl1*^{-/-}*3*^{+/-} naive mock treated with those from *Dvl1*^{-/-}*3*^{+/-} CHIR99021 treated and WT).



Supplementary Fig. 8: Embryonic activation of Wnt canonical pathway regulates embryonic β -catenin and Brn2 levels and adult behavior. a, Brains (E14.5) of WT and *Dvl* mutant embryos that were CHIR99021 or mock treated were immunostained using DAPI (blue), anti-Brn2 (green) and β -catenin (red) at

E14.5 (scale bar=100 μ m). Quantification of the number of nuclei (**b**), the levels of Brn2 (**c**) and levels of β -catenin (**d**) are presented as mean \pm SEM (* p <0.04 for comparison of the results from *Dvl1*^{-/-}*3*^{+/-} mock treated with those of WT mock treated embryos). **e**, Representative images of WT and *Dvl1*^{-/-}*3*^{+/-} mock and CHIR99021 treated mouse cages from the nest building test after 90 min. **f**, Social approach task in females was recorded and scored, results are presented as mean \pm SEM.

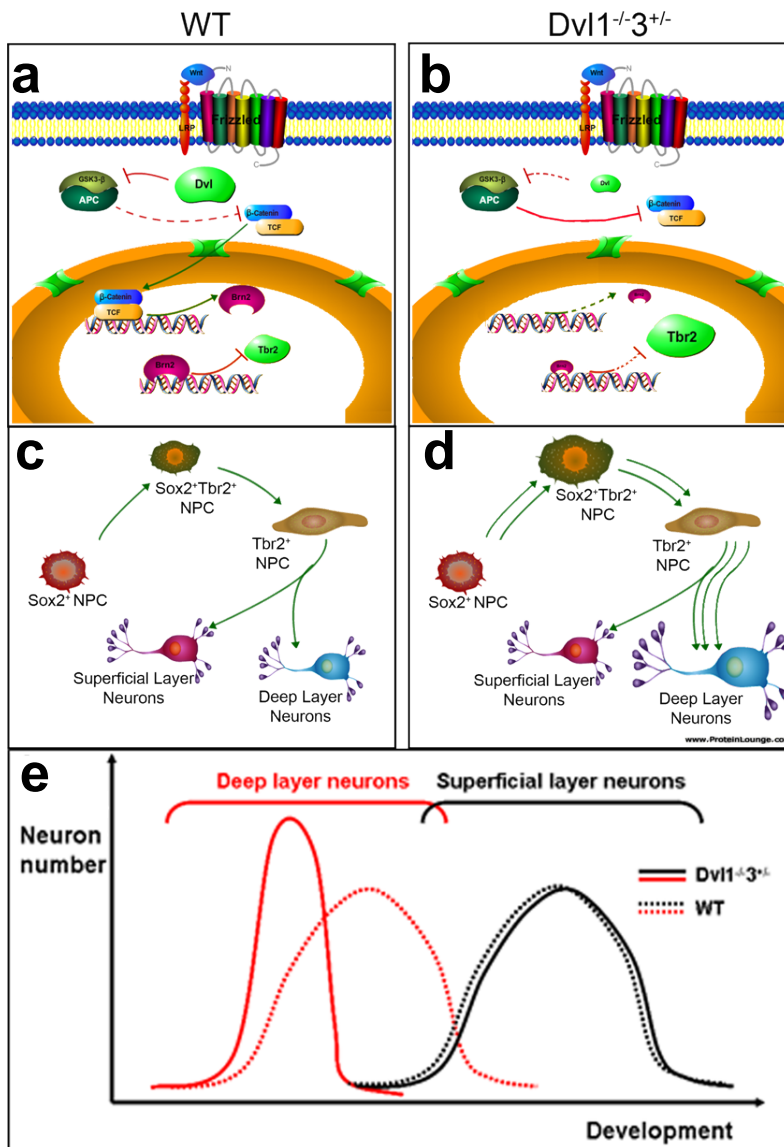


Supplementary Fig. 9: Embryonic activation of Wnt canonical pathway regulates adult brain structure. **a**, Relative volume voxelwise differences between the *Dvl1*^{-/-} CHIR vs. the *Dvl1*^{-/-} mock. The light red background is covering the areas in which there was a significant difference in relative volume between the *Dvl1*^{-/-} mock and WT mock. The stronger differences (i.e. differences which bring the CHIR KO closer to the WT mock) are represented by the spectral color-bar. Of the voxels which were significantly different between the *Dvl1*^{-/-} mock and WT mock in relative volume 74.7% of them trended towards recovery. **b**, Highlights the areas of significant interaction between the genotypes and treatment. There is a strong interaction found in the olfactory bulbs as well as a small bilateral interaction at the tip of the cerebral peduncle. **c-e**, Quantification of regions affected by volumetric and FA analysis. The indicated regions are presented as mean±SEM. OB= olfactory bulb, FAC= Frontal association cortex, (*p<0.05 for comparison of the results from *Dvl1*^{-/-} mock treated with those of the brackets indicated groups).

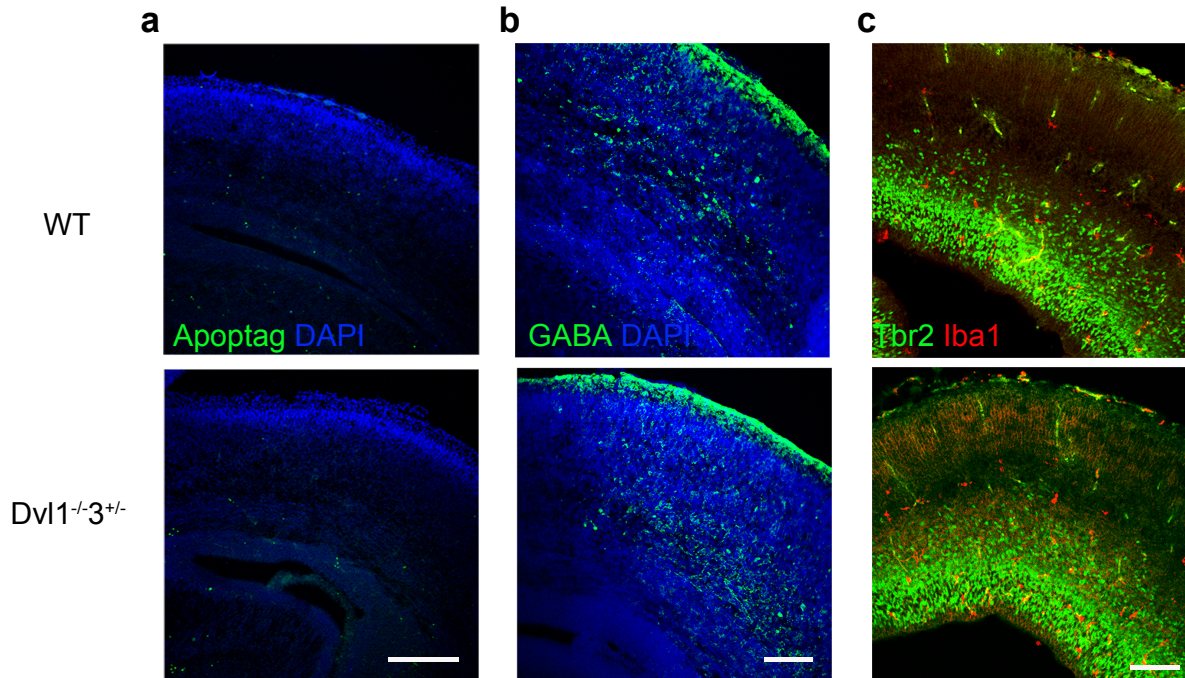
Supplementary Table 4: Volumetric analysis of 159 different regions examined in the brains of mock and CHIR99021 embryonically treated WT and *Dvl1*^{-/-} mice. The regions are listed as absolute volume and relative volume in % total brain volume. The mean and standard deviation (SD) of the volumes are listed. Also the percentage difference of the compared groups as well as the p-value and corresponding FDR value. - for FDR values of <10%, * for FDR values <5%, and ** for FDR values <1

Supplementary Table 5: Fractional Anisotropy (FA) analysis of 159 different regions examined in the brains of mock and CHIR99021 embryonically treated WT and *Dvl1*^{-/-} mice. The FA values for each region examined are presented as mean and standard deviation (SD) of the FA are listed. Also the percentage difference of the *Dvl1*^{-/-} compared with the WT mouse is calculated as well as the p-value and corresponding FDR value. - for FDR values of <10%, * for FDR values <5%, and ** for FDR values <1%.

Supplementary Table 6: Volumetric analysis of 159 different regions examined in the brains of WT mock and *Dvl1*^{-/-} CHIR99021 embryonically treated mice. The regions are listed as absolute volume and relative volume in % total brain volume. The mean and standard deviation (SD) of the volumes are listed. Also the percentage difference of the compared groups as well as the p-value and corresponding FDR value. - for FDR values of <10%, * for FDR values <5%, and ** for FDR values <1



Supplementary Fig. 10: Prenatal Wnt canonical pathway regulates Brn2/Tbr2 cascade and neuronal differentiation. a-e, Schematic representation of the molecular and cellular mechanism of proliferation and neurogenesis in WT and *Dvl* mutant mice and NPCs.



Supplementary Fig. 11: Mechanism for the rapid decrease in the deep layer neurons in the brains of *Dvl* mutants at E16.5. **a**, Coronal sections of WT, and *Dvl1^{-/-}3^{+/-}* embryo at E16.5 were stained with DAPI (Blue) and the apoptotic nuclei's detection system, Apoptag, and representative sections are presented (scale bar=100 μ m). **b**, Coronal sections of WT, and *Dvl1^{-/-}3^{+/-}* embryo at E18.5 were stained with DAPI (Blue) and anti-GABA antibody and representative sections are presented (scale bar=100 μ m). **c**, Coronal sections of WT, and *Dvl1^{-/-}3^{+/-}* embryo at E16.5 were stained with DAPI (Blue) anti-Tbr2 (green) anti-Iba1 (red) and representative sections are presented (scale bar=100 μ m).